

Numerical modelling of microcracking in PV modules
induced by thermo-mechanical loads

Original

Numerical modelling of microcracking in PV modules
induced by thermo-mechanical loads / Paggi, Marco; Sapora, ALBERTO GIUSEPPE. - In: ENERGY PROCEDIA. - ISSN
1876-6102. - 38:(2013), pp. 506-515. [10.1016/j.egypro.2013.07.310]

Availability:

This version is available at: 11583/2515097 since: 2016-05-06T14:49:23Z

Publisher:

Elsevier

Published

DOI:10.1016/j.egypro.2013.07.310

Terms of use:

This article is made available under terms and conditions as specified in the corresponding bibliographic description in the repository

Publisher copyright

(Article begins on next page)

SiliconPV: March 25-27, 2013, Hamelin, Germany

Numerical modelling of microcracking in PV modules induced by thermo-mechanical loads

Marco Paggi, Alberto Sapora

*Department of Structural, Geotechnical and Building Engineering, Politecnico di Torino,
Corso Duca degli Abruzzi 24, 10129 Torino, Italy*

Abstract

Micro-cracking in polycrystalline Silicon is a serious concern for the durability of photovoltaic (PV) modules due to the resulting electrical power-loss. In this contribution, a thermo-mechanical cohesive zone model is proposed to predict the evolution of micro-cracks under the action of mechanical and thermal loads. The classical nonlinear cohesive zone approach, used in fracture mechanics to depict the phenomenon of cracking as a result of progressive breakage of atomic bonds, is extended to thermo-elastic fields. The additional thermal resistance of micro-cracks due to imperfect bonding is estimated according to an analogy with a contact mechanics formulation, where the dependency on the crack opening is suitably accounted for. A numerical example shows the applicability of the proposed approach to practical problems.

© 2013 The Authors. Published by Elsevier Ltd. Open access under [CC BY-NC-ND license](#).

Selection and/or peer-review under responsibility of the scientific committee of the SiliconPV 2013 conference

Keywords: Photovoltaics; Thermoelasticity; Fracture Mechanics; Contact Mechanics; Computational methods.

1. Introduction

The problem of micro-cracking in Silicon PV has recently been investigated in [1-4] with the aid of the electroluminescence (EL) technique, which results a powerful method to detect electrically inactive cell areas and cracks. Due to the very brittle mechanical behavior of Silicon and the use of thin cells, cracks can be easily induced by vibrations, impacts during transportation, as well as by heavy snow pressure.

The development of a computational framework to model this phenomenon and understand its origin to propose new design solutions able to limit or even remove its effects is very important. For this research purpose, commercial finite element (FE) programs are quite limited in their capabilities, even if 3D geometries can be handled today due to the advancement in computer technology. A multi-scale and multi-physics computational model of the composite PV laminate, considering nonlinear fracture mechanics for simulating cracking in polycrystalline Silicon has been proposed in [5]. The methodology

is promising to predict the electrically disconnected cell areas (Fig. 1(a)) taking into account the actual polycrystalline geometry of Silicon cells (Fig. 1(b)). Although the methodology in [5] can be applied to realistic PV geometries, the effect of micro-cracking on the power-loss has been taken into account as a worst case scenario. In fact, all the numerically determined cracks have been considered as perfectly insulated. Therefore, according to the geometrical criterion proposed in [2], all the areas separated by micro-cracks are thermally insulated and electrically inactive (dark areas in Fig. 1(a)). This situation represents of course a limit case and a more refined model considering the actual thermal and electric conductivities of micro-cracks is envisaged to provide predictions closer to experiments.

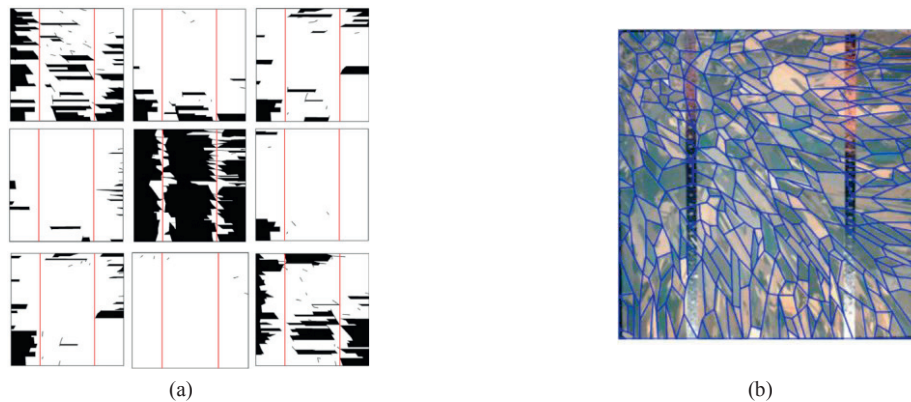


Fig. 1. Numerical simulation of cracking in a PV module composed of 3 x 3 Si cells subjected to snow pressure [5]. (a) Electrically disconnected cell areas (worst case scenario of electrically insulated cracks); (b) An image of one Si cell with grain boundaries in blue.

One of the main complexities of cracking in PV modules regards the contemporaneous presence of the elastic, thermal and electric fields with their essential coupling. The physics of the photovoltaic effect shows that the interplay between the electric and the thermal fields is not negligible. As a general trend, the current intensity-voltage (I-V) curves move towards lower voltages by increasing the cell temperature. From equivalent circuit models of PV modules with two diodes, a temperature increase from 10°C to 70°C reduces the open circuit voltage of about 20%. The coupling between the elastic and the thermal fields and between the elastic and the electric ones are also important but are much more difficult to be ascertain and modeled.

Experimental results [6,7] show that a micro-cracked cell presents a local increase of operating temperature near the crack. This effect can be qualitatively observed during operating conditions with an infrared (IR) thermal image, see Fig. 2(a). More quantitatively, dark lock-in thermography shows that micro-cracks are acting primarily as recombination centers with a local increase in temperature near the defect, see Fig. 2(b) compared with an EL image of the same damaged cell shown in Fig. 2(c).

At the continuum level, this phenomenon can be modeled by considering an additional thermal resistance of micro-cracks with respect to the situation of perfect bonding.

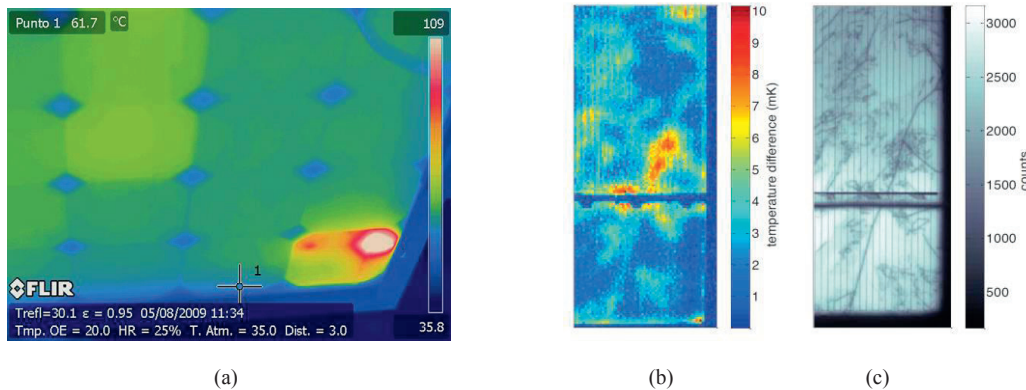


Fig. 2. (a) Thermal image showing a temperature increase in a defective cell [6]. (b) Dark lock-in thermography image of the temperature difference around a micro-crack [7]. (c) EL image of the same cell portion in (b) showing the crack pattern [7].

An interface constitutive law relating the thermal flux q normal to the interface to the temperature jump g_T across the crack faces has to be introduced:

$$q = -k_{\text{int}} g_T. \quad (1)$$

where k_{int} represents the interface conductivity. The Kapitza model, popular in nanoscale applications [8] suggests that k_{int} is just a constant. In reality, experimental results show a more complex behavior in case of PV applications. A detailed in situ monitoring of a micro-cracked cell –with 8% of cell area potentially electrically inactive– shows that the average cell temperature is not constant during the monitoring time (see Fig. 3 adapted from [9]). As compared to an intact cell, the temperature is higher and highly oscillating. At the same time, the output voltage of the string oscillates from 1V up to 9V. This behavior suggests that the detected micro-crack is not electrically insulated, but it is still able to conduct heat flux and electricity through its crack faces. Presumably, the recovery of electrical response (self-healing) is the result of closing of the crack faces due to thermo-elastic effects.

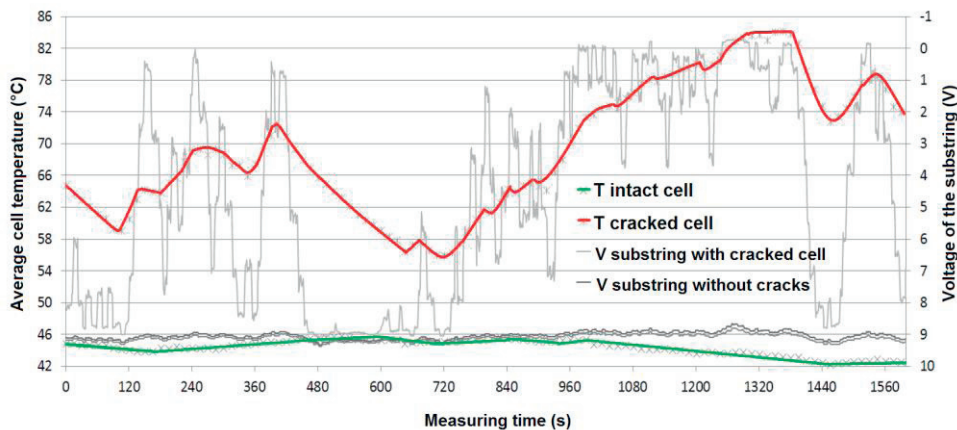


Fig. 3. Cell temperature and voltage of a substring with a micro-cracked cell vs. monitoring time, showing a highly oscillating response [9].

Motivated by the necessity of simulating how environmental aging promotes power-loss in PV modules, a new thermo-mechanical nonlinear fracture mechanics model is herein proposed. The key idea is to augment the physical description of the interface constitutive law of a micro-crack by considering the problem of heat conduction in addition to the transfer of mechanical tractions. With the aim of keeping the number of model parameters as low as possible to simplify their experimental identification, an approach inspired by a micromechanical contact model is proposed. As compared to previous attempts developed to model specific mechanical problems [10,11], the resulting formulation is more general and applies to any fracture problem leading to microscopically rough crack profiles.

2. A thermo-mechanical cohesive zone model inspired by contact mechanics

The progressive separation of an interface due to the propagation of a crack can be effectively modeled by the cohesive zone model (CZM) [12]. The CZM establishes a relation between the normal (Mode I) and tangential (Mode II) cohesive tractions and the relative opening and sliding displacements experienced by the two opposite crack surfaces. Inspired by atomic potentials, different shapes of the CZM have been proposed so far, see the sketches in Fig. 4 [12]. The various formulations for a pure Mode I problem are characterized by the peak cohesive traction, σ_{\max} , and the Mode I fracture energy, G_{IC} , which is the area under the CZM curve. When the opening displacement equals a critical separation, g_{nc} , a stress-free crack is created. Linear or bilinear softening CZMs are usually selected in case of brittle materials, whereas trapezoidal or bell-shape CZMs are used in case of ductile fracture. In some cases, linear and bilinear CZMs have an initial elastic branch with very high stiffness. This branch is necessary when interface elements are inserted from the very beginning of the numerical simulations along pre-defined crack paths.

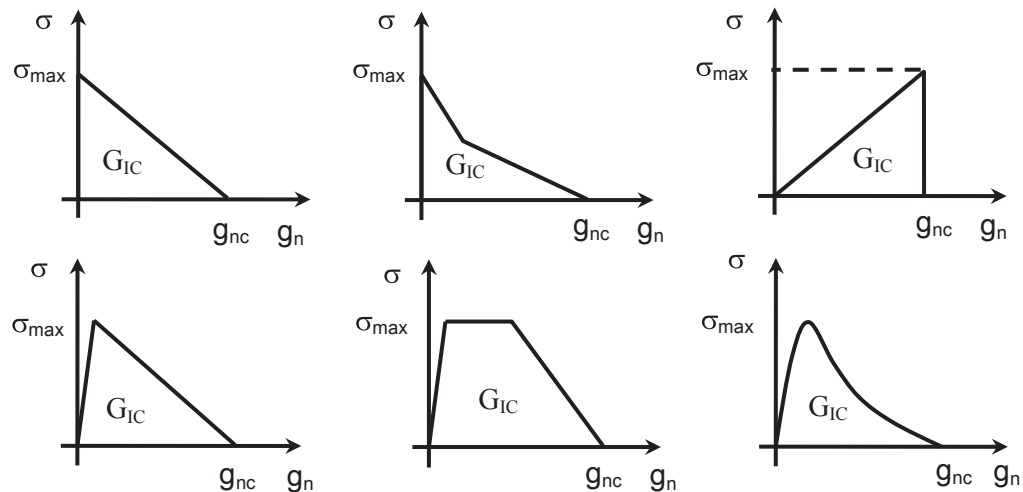


Fig. 4. Qualitative comparison between the shapes of the CZMs available in the literature.

The extension of the basic CZM formulation valid for mechanical loading to thermo-elastic problems led to the so-called thermo-mechanical CZMs [10,11]. In addition to the relation between normal and tangential cohesive tractions and opening and sliding displacements, an equation relating the thermal flux across the crack faces and the temperature jump of the type (1) is introduced.

In the present work, a new thermo-mechanical CZM is proposed based on contact mechanics principles. It is in fact well-known that, in case of contact between two bodies with rough boundaries, a temperature jump takes place at the bi-material interface. The heat flux is related to the temperature jump by micromechanical relations. In case of elastic contact, the fundamental theorem by Barber [13] suggests that the contact conductance due to roughness is proportional to the normal contact stiffness. Hence, taking advantage of this result, it is possible to estimate the interface contact conductance directly from the solution of the normal contact problem, without the need of introducing *ad hoc* independent constitutive relations for the thermal response. In general, since the contact stiffness is dependent on the applied pressure, a separation-dependent interface contact conductance is obtained [14].

In the present problem, where the thermo-mechanical CZM should depict the phenomenon of decohesion, an analogy with contact mechanics can be put forward. During contact, a compressive pressure p (negative valued) is applied to the rough surface and it ranges from zero (first point of contact) to the full contact pressure, p_{FC} , see Fig. 5. In case of fracture, the process is reversed. The full contact regime corresponds to an intact interface. In this situation, to separate the two bodies and create a stress-free crack, a tensile pressure (positive) and equal in modulus to p_{FC} has to be applied. The process of debonding is not sudden and it progressively produces a rough surface which finally leads to the microscopically rough stress-free crack (from left to right in Fig. 5).

Hence, the Mode I cohesive traction σ which, by definition, is the traction opposed to crack opening, can be evaluated at any mean plane separation g_n as the opposite of the applied contact pressure p corresponding to the same separation.

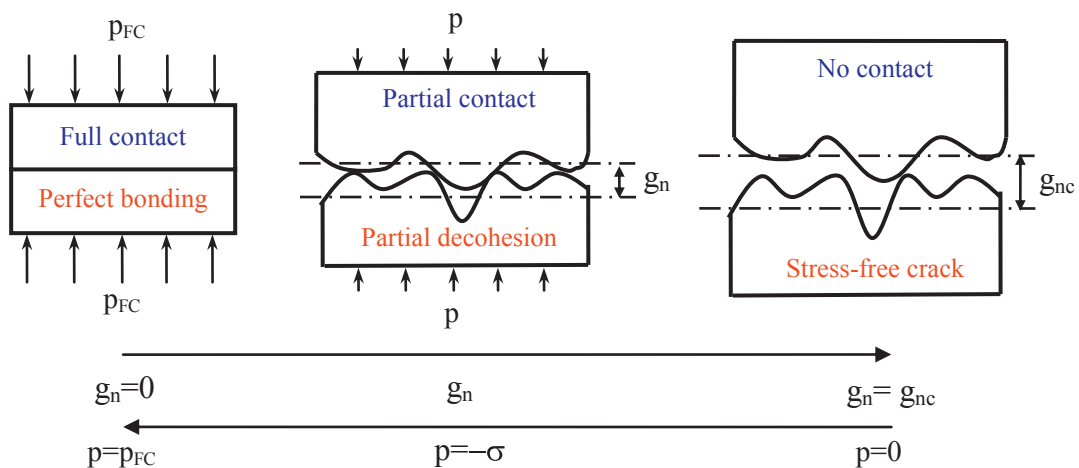


Fig. 5. Analogy between contact mechanics and fracture mechanics.

Among the possible pressure-separation relations established in the literature for a rough interface, the exponential model by Greenwood and Williamson [15] is adopted. Considering an exponential distribution of asperity heights with a root mean square “rms”, an exponential decay of the cohesive traction is expected for $g_n \geq l_0$. A linear regularization for $0 \leq g_n < l_0$ is introduced here primarily for numerical reasons, since interface elements will be inserted between the finite elements from very the beginning of the simulation.

For separations larger than g_{nc} , a cut-off to the cohesive tractions corresponding to the formation of a stress-free crack is introduced. To consider the weakening effect of Mixed-Mode deformation, the tangential gap g_t is also introduced in the formulation. The resulting expression for the normal cohesive traction is the following:

$$\sigma = \begin{cases} \sigma_{\max} \exp\left(\frac{-l_0 - g_t}{\text{rms}}\right) \frac{g_n}{l_0} & \text{if } 0 \leq \frac{g_n}{\text{rms}} < \frac{l_0}{\text{rms}} \\ \sigma_{\max} \exp\left(\frac{-g_n - g_t}{\text{rms}}\right) & \text{if } \frac{l_0}{\text{rms}} \leq \frac{g_n}{\text{rms}} < \frac{g_{nc}}{\text{rms}} \\ 0 & \text{if } \frac{g_n}{\text{rms}} \geq \frac{g_{nc}}{\text{rms}} \end{cases} \quad (2)$$

And a similar relation can be proposed for the Mode II tangential cohesive tractions:

$$\tau = \begin{cases} \tau_{\max} \exp\left(\frac{-l_0 - g_n}{\text{rms}}\right) \frac{g_t}{l_0} & \text{if } 0 \leq \frac{g_t}{\text{rms}} < \frac{l_0}{\text{rms}} \\ \tau_{\max} \exp\left(\frac{-g_t - g_n}{\text{rms}}\right) & \text{if } \frac{l_0}{\text{rms}} \leq \frac{g_t}{\text{rms}} < \frac{g_{tc}}{\text{rms}} \\ 0 & \text{if } \frac{g_t}{\text{rms}} \geq \frac{g_{tc}}{\text{rms}} \end{cases} \quad (3)$$

The Mode I cohesive traction (2) is plotted vs. the opening relative displacements in Fig. 6(a). The interface contact conductance can now be determined via the derivative of the normal pressure-separation relation:

$$k_{\text{int}} = \begin{cases} \frac{1}{\rho_{\text{int}}} & \text{if } 0 \leq \frac{g_n}{\text{rms}} < \frac{l_0}{\text{rms}} \\ \frac{2\sigma}{\rho_{\text{int}} E_{\text{int}} \text{rms}} & \text{if } \frac{l_0}{\text{rms}} \leq \frac{g_n}{\text{rms}} < \frac{g_{nc}}{\text{rms}} \\ 0 & \text{if } \frac{g_n}{\text{rms}} \geq \frac{g_{nc}}{\text{rms}} \end{cases} \quad (4)$$

The resistivity ρ_{int} and the Young's modulus E_{int} of the interface can be evaluated as $\rho_{\text{int}} = \rho_1 + \rho_2$ and $E_{\text{int}} = [(1-\nu_1^2)/E_1 + (1-\nu_2^2)/E_2]^{-1}$, where the subscripts 1 and 2 refer to the materials separated by the interface and ν is the Poisson's ratio. In the linear range $0 \leq g_n < l_0$, a constant interface conductivity is selected. Since the maximum interface conductivity in contact problems can be attained for a small

separation larger than zero, the parameter l_0 can be selected according to this physical argument. In PV applications, l_0 is of the order of $\text{rms}/100$.

It is interesting to note the similitude between the present formulation deduced according to contact mechanics considerations and the CZM by Xu and Needleman [16]. In [16], the shape of the CZM is the result of the product between a linear function of the gap (dominating for small separations) and an exponential decay (prevailing for large separations), see the dashed curve in Fig. 6(a). However, this CZM leads to a convex shape in the range $0 \leq g_n < \text{rms}$ which provides unrealistic values for the interface contact conductance if computed from the normal contact stiffness (see Fig. 6(b), where a comparison among the proposed CZM and that by Xu and Needleman is proposed considering $l_0/\text{rms}=0.5$ for a better visualization). Moreover, the main advantage of the proposed formulation relies in the fact that the thermal part of the CZM does not involve other model parameters than the bulk thermal resistance and the Young's modulus, easy to be experimentally evaluated. Finally, it has to be remarked that the interface conductance (4) does depend on the separation and it is not just a mere constant as in the Kapitza model.

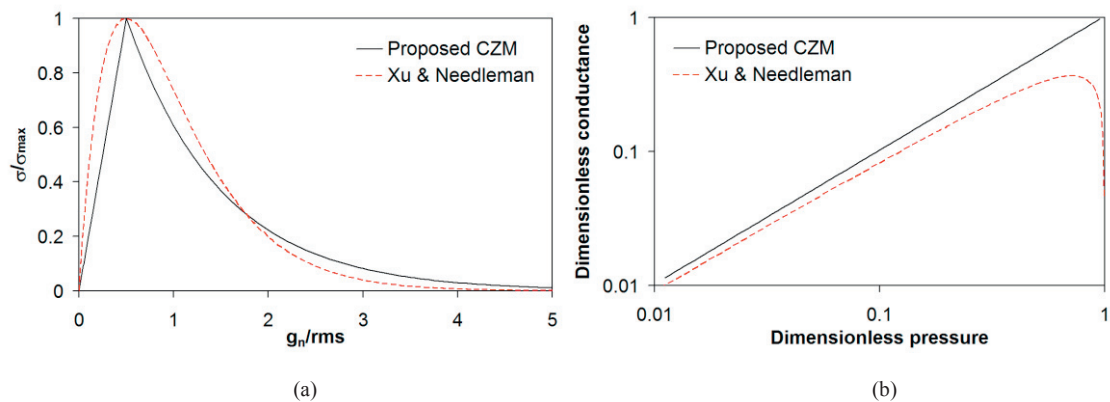


Fig. 6. (a) Mode I CZM proposed in the present work and the CZM by Xu and Needleman [16]. (b) Dimensionless conductance vs. dimensionless pressure obtained by differentiating the CZMs in Fig. 6(a).

3. Weak form of the problem, solution methods and numerical example

In the most general case, the coupling between the elastic and the thermal fields can be accounted for by considering the equations of thermo-elasticity for the continuum and the Fourier heat conduction equation $\mathbf{q} = -k\nabla T$, being ∇ the gradient operator. Microcracks introduce an additional thermal resistance with respect to that of the continuum, which is associated to imperfect bonding. The numerical implementation of the CZM in the finite element method comes from the weak form of the balance equations. By considering a body with volume V and surface ∂V , for what concerns the mechanical problem we have:

$$\int_V \boldsymbol{\sigma}^T (\nabla \delta \mathbf{u}) dV = \int_V \mathbf{f}^T (\delta \mathbf{u}) dV + \int_{\partial V} \bar{\boldsymbol{\sigma}}^T (\delta \mathbf{u}) dS + \int_S \mathbf{t}^T (\delta \mathbf{g}) dS \quad (5)$$

where $\boldsymbol{\sigma}$ is the stress vector, \mathbf{u} is the displacement vector, \mathbf{f} is the body force vector, $\bar{\boldsymbol{\sigma}}$ is the vector of prescribed tractions on the boundary, $\mathbf{t} = (\tau, \sigma)^T$ and $\mathbf{g} = (g_t, g_n)^T$. On the other hand, as regards the thermal problem we can write (transient regime in absence of internal heat sources):

$$\int_V \mathbf{q}^T (\nabla \delta T) dV = \int_V \rho_V c_V \dot{T} \delta T dV + \int_{\partial V} \bar{q} \delta T dS + \int_S q \delta g_T dS \quad (6)$$

where ρ_V is the mass density, c_V is the specific heat and \bar{q} is the vector of prescribed normal heat fluxes.

Notice that the last terms on the right hand sides of Eqs. (5) and (6) are the additional contributions related to the cohesive crack surfaces S . Since the cohesive tractions \mathbf{t} are nonlinear functions of the opening and sliding displacements \mathbf{g} , Eq. (5) is nonlinear. The same applies to Eq. (6), where the heat flux q is a nonlinear function of the thermal gap g_T via the interface contact conductance. Coupling the mechanical and thermal fields comes from the influence of temperature on the deformation of the continuum, as well as on the dependency of the interface conductance on the crack opening displacement. Considering interface elements with linear shape functions interpolating the nodal displacements and temperatures as in [17], the Newton-Raphson solution method has to be adopted to consistently linearize the set of equations. For more details, the reader is referred to [11,17].

Here, we consider a preliminary test problem consisting of a solar cell with length 0.125 m, with an ideal micro-crack parallel to the busbar and placed at a distance 0.03 m from the left side (Fig. 7(a)). This is a possible crack pattern of cells close to the border of the panel, in a middle position far from the panel corners (Fig. 7(b)). The continuum is modeled by plane stress quadrilateral finite elements with linear shape functions and a thickness equal to 1.66×10^{-4} m. The thermo-elastic parameters are $E = 169 \times 10^9$ Pa, $\nu = 0.16$, $\rho_V = 3100$ kg/m³, $k = 114$ W/m°C, $c_V = 715$ J/kg°C. The coefficient of thermal expansion is taken equal to $\alpha = 1.1 \times 10^{-6}$ /°C. Regarding the micro-crack, the cohesive peak stress is $\sigma_{\max} = 190 \times 10^6$ Pa, whereas the fracture energy is $G_{IC} = 5.92$ N/m. From these values we can deduce the value of $g_{nc} = 0.2 \times 10^{-6}$ m, $rms = 3.135 \times 10^{-8}$ m, and $l_0 = 3.135 \times 10^{-10}$ m.

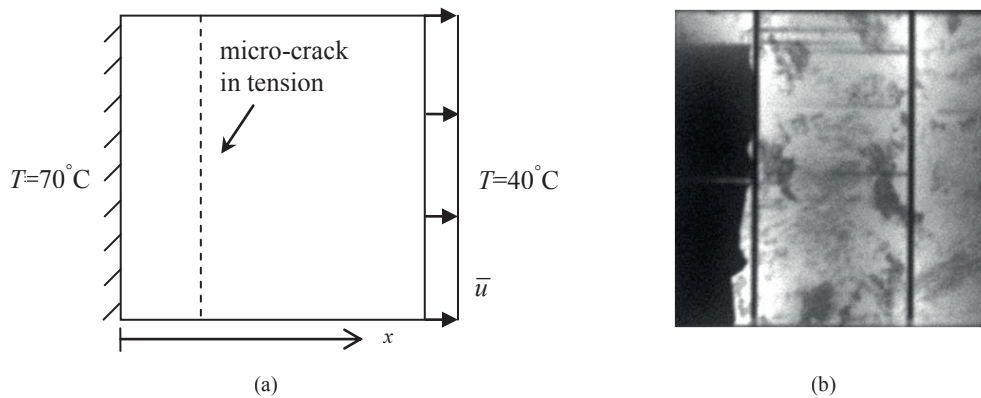


Fig. 7. (a) Sketch of a solar cell with a micro-crack: boundary conditions for the thermo-elastic analysis are shown. (b) EL image of a damaged solar cell.

To simulate the effect of cracking on this boundary cell induced by the self-weight of the panel, a horizontal displacement \bar{u} estimated from the finite element solution of the composite plate subjected to a uniform distributed loading [5] is applied to the right hand side of the cell boundary. This imposed displacement induces a crack opening of 1.35×10^{-7} m. At this point, a thermo-elastic problem is solved. A temperature of 70°C is applied to the left boundary of the cell, whereas a temperature of 40°C is imposed to the opposite side. This is to simulate the increase of temperature in the domain partially insulated from the rest of the cell from the electrical point of view, as also observed in experiments [9]. The geometry of the micro-crack and the boundary conditions lead to a quasi mono-dimensional problem. In this case,

examining the quasi-static regime, a solution can be gained via direct integration of the balance differential equations (strong form of Eqs. (5) and (6)). A staggered solution scheme is also appropriate due to the weak coupling (one single interface). The mechanically induced crack opening is used to compute the thermal conductance of the crack via Eq. (4). Then, the heat conduction equation is solved by considering the temperature boundary conditions above, the continuity of the heat flux at the interface and the relation between temperature gap and heat flux at the crack due to the interface thermal conductance. From the computed temperature distribution, the thermal expansion leads to a decrease in crack opening. Hence, an updated cohesive traction is computed for the new gap and the thermal problem is solved again with an updated interface thermal conductance. This procedure is iterated until convergence is achieved.

The result of this staggered scheme is depicted in Fig. 8. The temperature distribution for various iterations is shown in Fig. 8(a). At convergence, the initial temperature jump of 30°C that would correspond to a perfectly insulated crack, is slightly reduced due to the fact that the crack conductance is not zero. The crack opening, on the other hand, reduces significantly due to thermal expansion of the continuum and, after about 10 iterations, it converges down to $0.115\text{ }\mu\text{m}$ (Fig. 8(b)).

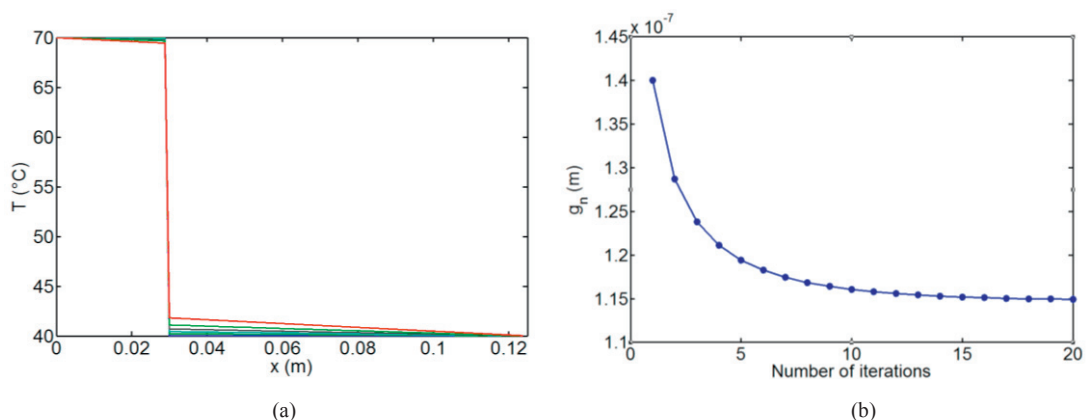


Fig. 8. (a) Temperature distribution during the simulation (the red curve in the online version corresponds to the solution at convergence). Note the temperature jump at the crack location. A vanishing interface thermal conductance (perfect insulation of the micro-cracked cell) would result in a sharp jump of 30°C . (b) Evolution of the crack opening displacement vs. number of iterations.

4. Concluding remarks

A thermo-mechanical CZM inspired by contact mechanics between rough surfaces has been proposed in this study. A preliminary application to Silicon cells has shown that thermo-elastic effects are quite complex. Temperature differences between the damaged and the intact portions of a solar cell can induce a significant reduction of crack opening. For small cracks, this phenomenon can induce crack closure and a self-healing of the crack with an increase of thermal conductance. Future perspectives of this work regard the numerical solution of 2D problems in the presence of multiple micro-cracks. In this case, the advantage of using a fully coupled solution scheme instead of a staggered one is envisaged to be useful for avoiding convergence problems, especially in case of a snapping from opening to closing configurations for small micro-cracks. Finally, coupling between the electric and the thermal fields has to be investigated. This is essential for modelling heat sources related to electron recombination effects and for comparing numerical predictions and experimental voltage data as in Fig. 3.

Acknowledgements

The research leading to these results has received funding from the European Research Council under the European Union's Seventh Framework Programme (FP/2007–2013)/ERC Grant Agreement No. 306622 (ERC Starting Grant “Multi-field and multi-scale Computational Approach to Design and Durability of PhotoVoltaic Modules” – CA2PVM). The support of the Italian Ministry of Education, University and Research to the Project FIRB 2010 Future in Research “Structural mechanics models for renewable energy applications” (RBFR107AKG) is also gratefully acknowledged.

References

- [1] Kajari-Schröder S, Kunze I, Eitner U, Köntges M. Spatial and orientational distribution of cracks in crystalline photovoltaic modules generated by mechanical load tests. *Solar Energy Mater Solar Cells* 2011; **95**:3054–3059.
- [2] Köntges M, Kunze I, Kajari-Schröder S, Breitenmoser X, Bjørneklett B. The risk of power loss in crystalline silicon based photovoltaic modules due to microcracks. *Solar Energy Mater Solar Cells* 2011; **95**:1131–1137.
- [3] Kajari-Schröder S, Kunze I, Köntges M. Criticality of cracks in PV modules. *Energy Procedia* 2012; **27**:658–663.
- [4] Khatir R, Agarwal S, Saha I, Singh SK, Kumar B. Study on long term reliability of photo-voltaic modules and analysis of power degradation using accelerated aging tests and electroluminescence technique. *Energy Procedia* 2011; **8**:396–401.
- [5] Paggi M, Corrado M, Rodriguez MA. A multi-physics and multi-scale numerical approach to microcracking and power-loss in photovoltaic modules. *Composite Structures* 2013; **95**:630–638.
- [6] Munoz MA, Alonso-Garcia MC, Vela N, Chenlo F. Early degradation of silicon PV modules and guaranty conditions. *Solar Energy* 2011; **85**:2264–2274.
- [7] van Mülken JI, Yusufoglu UA, Safiei A, Windgassen H, Khandelwal R, Pletzer TM, Kurz H. Impact of micro-cracks on the degradation of solar cell performance based on two-diode model parameters. *Energy Procedia* 2012; **27**:167–172.
- [8] Shahil KMF, Balandin AA. Graphene–multilayer graphene nanocomposites as highly efficient thermal interface materials. *Nano Letters* 2012; **12**:861–867.
- [9] Weinreich B, Schauer B, Zehner M, Becker G. Validierung der Vermessung gebrochener Zellen im Feld mittels Leistungs PV-Thermographie. In: *Tagungsband 27. Symposium Photovoltaische Solarenergie*, Bad Staffelstein, Germany, 2012, 190–196.
- [10] Özdemir I, Brekelmans WAM, Geers MGD. A Thermo-mechanical cohesive zone model. *Computational Mechanics* 2010; **26**:735–745.
- [11] Hattiangadi A, Siegmund T. A thermomechanical cohesive zone model for bridged delamination cracks. *Journal of the Mechanics and Physics of Solids* 2004; **52**:533–566.
- [12] Paggi M, Wriggers P. A nonlocal cohesive zone model for finite thickness interfaces – Part I: mathematical formulation and validation with molecular dynamics. *Computational Materials Science* 2011; **50**:1625–1633.
- [13] Barber JR. Bounds on the electrical resistance between contacting elastic rough bodies. *Proceedings of the Royal Society of London Ser. A* 2003; **459**:53–66.
- [14] Paggi M, Barber JR. Contact conductance of rough surfaces composed of modified RMD patches. *International Journal of Heat and Mass Transfer* 2011; **4**:4664–4672.
- [15] Greenwood JA, Williamson JBP. Contact of nominally flat surfaces. *Proceedings of the Royal Society of London Ser. A* 1966; **295**:300–319.
- [16] Xu X, Needleman A. Numerical simulations of fast crack growth in brittle solids. *Journal of the Mechanics and Physics of Solids* 1994; **42**:1397–1434.
- [17] Paggi M, Wriggers P. A nonlocal cohesive zone model for finite thickness interfaces – Part II: FE implementation and application to polycrystalline materials. *Comp. Mat. Sci.* 2012; **50**:1634–1643.